molecules

MDPI

*Article*

# Fast Determination of Eleven Food Additives in River Water Using C18 Functionalized Magnetic Organic Polymer Nanocomposite Followed by High-Performance Liquid Chromatography

**Chao Lei [1], Shun Zhang [2], Wen-Xin Liu [1,3], Ming-Li Ye [1,*] and Yong-Gang Zhao [1,*]**

[1] College of Biological and Environmental Engineering, Zhejiang Shuren University, Hangzhou 310015, China; chaolei_212@163.com (C.L.); lwx187221@163.com (W.-X.L.)
[2] Guoke Ningbo Life Science and Health Industry Research Institute, Ningbo 315010, China; zhangshun@ucas.ac.cn
[3] College of Environment, Zhejiang University of Technology, Hangzhou 310014, China
* Correspondence: 601279@zjsru.edu.cn (M.-L.Y.); zhyg91213@163.com (Y.-G.Z.)

**Abstract:** A novel magnetic nanomaterial with $Fe_3O_4$ as the core, PS-DVB as the shell layer, and the surface modified with C18 (C18−PS−DVB−$Fe_3O_4$) had been synthesized by seeded emulsion polymerization. C18−PS−DVB−$Fe_3O_4$ retains the advantages of the chemical stability, large porosity, and uniform morphology of organic polymers and has the magnetic properties of $Fe_3O_4$. A simple, flexible, and efficient magnetic dispersive solid phase extraction (Mag-dSPE) method for the extraction of preservatives, sweeteners, and colorants in river water was established. C18−PS−DVB−$Fe_3O_4$ was used as an adsorbent for Mag-dSPE and was coupled with high-performance liquid chromatography (HPLC) to detect 11 food additives: acesulfame, amaranth, benzoic acid, tartrazine, saccharin sodium, sorbic acid, dehydroacetic acid, sunset yellow, allura red, brilliant blue, and erythrosine. Under the optimum extraction conditions, combined with ChromCoreTMAQC18 (5 μm, 4.6 × 250 mm), 20 mmol/L ammonium acetate aqueous solution and methanol were used as mobile phases, and the detection wavelengths were 240 nm and 410 nm. The limits of detection (LODs) of 11 food additives were 0.6–3.1 μg/L with satisfactory recoveries ranging from 86.53% to 106.32%. And the material could be reused for five cycles without much sacrifice of extraction efficiency. The proposed method has been used to determine food additives in river water samples, and results demonstrate the applicability of the proposed C18−PS−DVB−$Fe_3O_4$ Mag-dSPE coupled with the HPLC method to environment monitoring analysis.

**Keywords:** magnetic dispersive solid phase extraction; food additives; high-performance liquid chromatography; magnetic nanomaterial

check for updates

**Citation:** Lei, C.; Zhang, S.; Liu, W.-X.; Ye, M.-L.; Zhao, Y.-G. Fast Determination of Eleven Food Additives in River Water Using C18 Functionalized Magnetic Organic Polymer Nanocomposite Followed by High-Performance Liquid Chromatography. *Molecules* **2024**, *29*, 3675. https://doi.org/10.3390/molecules29153675

Academic Editor: Dimitrios Bikiaris

Received: 30 June 2024
Revised: 27 July 2024
Accepted: 31 July 2024
Published: 2 August 2024

**Copyright:** © 2024 by the authors. Licensee MDPI, Basel, Switzerland. This article is an open access article distributed under the terms and conditions of the Creative Commons Attribution (CC BY) license (https://creativecommons.org/licenses/by/4.0/).

## 1. Introduction

With the increasing pursuit of an improved quality of life, people have much higher requirements for the quality of food. In order to improve the appearance, flavor, taste, and storage of food, food additives are usually used in the food industry [1]. These food additives, according to their function, can be divided into colorants, preservatives, sweeteners, thickeners, emulsifiers, enhancers, and acidity regulators, etc. [2–4]. The rational use of these food additives not only improves the color and taste of food, but also improves the nutritional value. However, the improper use of some food additives has led to potential threats to human health. In addition, some food additives have been shown to be potential causes of disease [5–7]. For example, Lakshmi and co-workers found that isatins may cause permanent damage to the cornea and conjunctiva [8]. Ma and co-workers reported that excessive intake of isatin has mutagenic effects and may lead to tumors. In addition, some highly toxic synthetic chemicals are also used as illegal

food additives, causing serious food safety accidents [9]. In addition, in the production, processing, packaging, transportation, and storage of food additives, food additives will flow into the environment due to improper operation [10]. Benzoic acid, which is often used for food preservation, was detected in groundwater at concentrations of 10~27,500 μg/L [11]. Acesulfame is used to improve the taste of food, and the concentration detected in surface water can be as high as 21 μg/L [12]. In addition, allura red, which is used for food coloring, was detected in natural water samples at concentrations ranging from 9.9 to 77.5 μg/L [13]. Therefore, the adsorption removal and enrichment detection of food additives in environmental water samples is an urgent problem to be solved.

In the production, processing, packaging, transportation, and storage of food additives, food additives will flow into the environment because of improper operation. In addition, many synthetic food additives are difficult to degrade in the body, and they are released into the environment through excretion. The ultimate destination of these food additives would be transferred to the surface water. And the decomposition of a variety of aromatic amines display carcinogenicity. Therefore, it is worth studying to establish a simple and feasible method for the detection of food additives in environmental water samples [14–17].

At present, the detection methods of food additives include liquid chromatography [18–22], gas chromatography [23], and colorimetric methods [24]. However, the composition of the sample is very complex, and the sample needs to be pretreated before the instrument detection. Solid phase extraction (SPE) is the most widely used pretreatment technique. It includes solid phase microextraction (SPME), dispersed-solid phase extraction (d-SPE) [25], and molecularly imprinted solid phase extraction (MISPE) [26–28]. SPE minimizes matrix effects, improves selectivity and recovery, and the detection limit of the instrument is greatly reduced [29]. In 2022, a novel molecularly imprinted polymer was used as an adsorbent for MISPE to remove sodium saccharin from the sample. The detection limit was 7.0 g/L [30]. SPE is more efficient and flexible than liquid–liquid extraction in terms of flexibility, simplicity, and low consumption of organic solvents. Still, the solid–liquid separation time is long after the target is adsorbed by the adsorbent. Therefore, an obvious trend in analytical chemistry is to shorten the separation time. To solve this problem, a simple and efficient magnetic dispersive solid phase extraction (Mag-dSPE) technique is developed. Mag-dSPE has the advantages of rapid solid–liquid separation, a simple method, and low cost, and it is suitable for complex matrices. The use of Mag-dSPE greatly reduces the consumption of organic solvents, which is an environmentally friendly technology [31–34]. So, Mag-dSPE is also widely used in the pretreatment of food additives in recent years [35–39]. In 2020, a novel magnetic porous nanofiber was used as an adsorbent for Mag-dSPE and HPLC to detect Sudan dye in food, with a detection limit of 0.88–1.27 μg/L [40].

In this study, in order to improve the preferential adsorption ability of magnetic nanomaterials to weak polar or non-polar compounds, the materials were modified by C18. C18 modification is a commonly used functional method in reversed-phase chromatography. The working principle of reversed-phase chromatographic packing is to separate the components of a chemical mixture at an appropriate flow rate by making use of the difference in affinity between chemical substances with different chemical phases and fillers. Its separation is based on the difference between the hydrophilicity and hydrophobicity of compounds. Therefore, after the modification of C18, the specific adsorption ability of the material to non-polar compounds was increased.

At present, C18 materials are mainly silicon-based materials. Compared with organic resin, silicon-based materials have no advantage in preparation or cost. In order to prepare a kind of material which can replace silicon-based C18 material, a novel magnetic nanomaterial with $Fe_3O_4$ as the core, PS-DVB as the shell layer, and the surface modified with C18 (C18−PS−DVB−$Fe_3O_4$) was synthesized. C18−PS−DVB−$Fe_3O_4$ is used as a powerful sorbent in Mag-dSPE for the separation and preconcentration of 11 food additives. In addition, an analytical procedure combining the Mag-dSPE technique with HPLC has been proposed (Figure 1). The excellent sensitivity of the developed method for 11 food

additives was investigated in laboratory batch tests, and it can be applied to the routine analyses for the determination of food additives in environmental water samples.

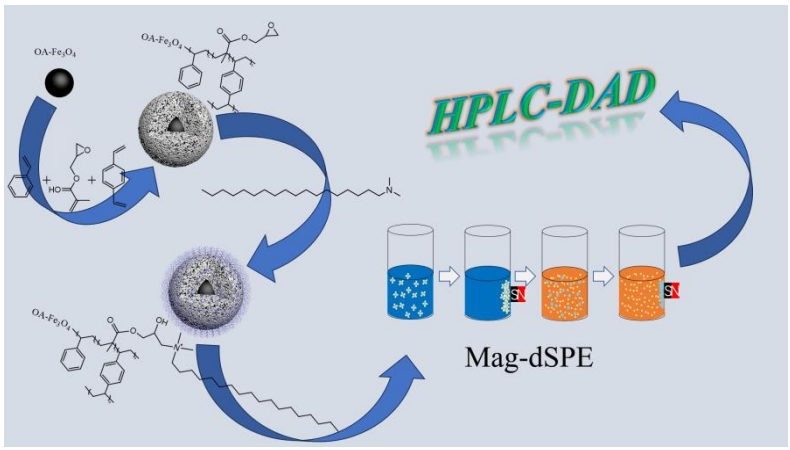


**Figure 1.** Preparation of C18−PS−DVB−$Fe_3O_4$ and the Mag-dSPE process.

## 2. Results and Discussion

### *2.1. Characterization of C18−PS−DVB−$Fe_3O_4$*

In this study, a novel nanomaterial of C18−PS−DVB−$Fe_3O_4$ was synthesized, and the excellent properties of C18−PS−DVB−$Fe_3O_4$ were characterized by SEM, VSM, XPS, and BET.

#### 2.1.1. Morphological Characteristics

The morphological features of $Fe_3O_4$ and C18−PS−DVB−$Fe_3O_4$ were investigated by SEM and TEM. As shown in Figure 2a, the SEM image exhibited that the particle size of $Fe_3O_4$ was uniform. The C18−PS−DVB−$Fe_3O_4$ nanoparticles had a good spherical shape, a smooth surface, and many pores. Combined with the Figures 2b,c and 3, the uniformity of the particle size needs to be improved. However, C18−PS−DVB−$Fe_3O_4$ presented an image of the core-shell structure. This was because the electron beam was difficult to pass through $Fe_3O_4$, but it can pass through organic resin.

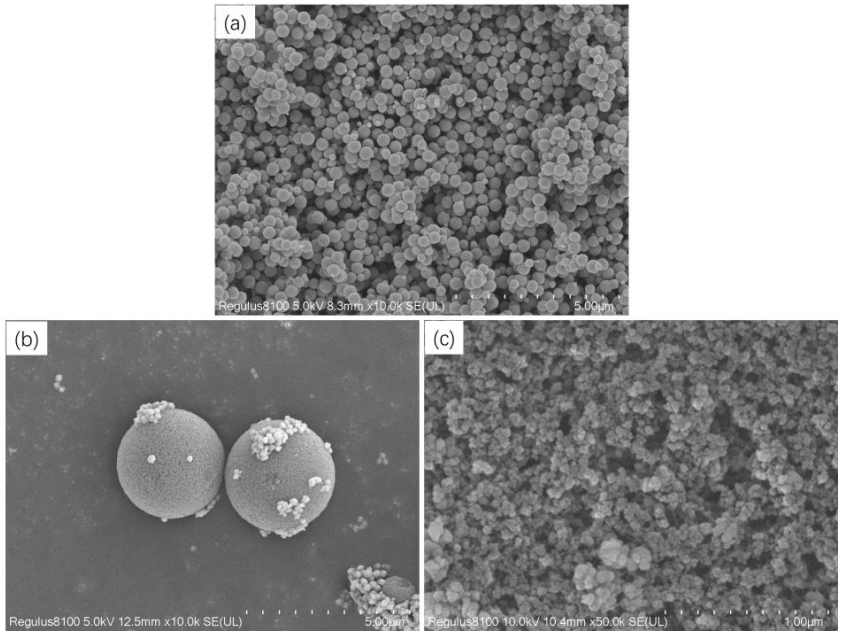


**Figure 2.** SEM images of nano $Fe_3O_4$ (**a**), C18−PS−DVB−$Fe_3O_4$ (**b**), and a high-definition picture of C18−PS−DVB−$Fe_3O_4$ (**c**).

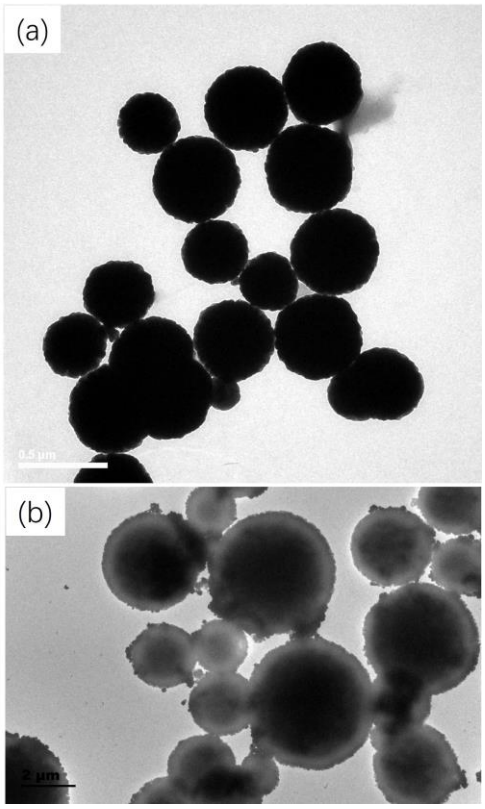


**Figure 3.** TEM images of $Fe_3O_4$ (**a**) and C18−PS−DVB−$Fe_3O_4$ (**b**).

2.1.2. Magnetic Property

Figure 4 showed the magnetic performance of $Fe_3O_4$ and C18−PS−DVB−$Fe_3O_4$, which were analyzed by VSM. The magnetic hysteresis loops reflect that the saturation value of $Fe_3O_4$ was 62.67 emu/g, and C18−PS−DVB−$Fe_3O_4$ was 19.93 emu/g. The saturation magnetization of C18−PS−DVB−$Fe_3O_4$ was obviously lower than that of $Fe_3O_4$, which was related to the organic polymer layer that coated the $Fe_3O_4$ surface effectively. However, it had no remarkable influence on the rapid magnetic separation of the adsorbent from the sample solution. C18−PS−DVB−$Fe_3O_4$ can not only be evenly dispersed in a solution without an external magnetic field, but can also be rapidly separated from the solution via a magnet within 10 s.

2.1.3. XPS Analysis

The chemical composition of C18−PS−DVB−$Fe_3O_4$ was investigated by XPS. As shown in Figure 5a, the wide scan XPS spectra showed photoelectron lines at a binding energy of about 284.18 eV and 532.12 eV, attributed to carbon (C1s) and oxygen (O1s). The C1s high-resolution scan could be fitted into four peaks (Figure 5b) with binding energies of 283.68 eV, 284.18 eV, 286.08 eV, and 288.08 eV, which were attributed to C-N, C-H, C-O, and O-C=O, respectively. The O1s high-resolution scan could be fitted into three peaks (Figure 5c) with binding energies of 529.42 eV, 531.62 eV, and 532.57 eV, which were attributed to O-H, O=C, and C-O, respectively. The successful functionalization was affirmed by the appearance of an N1s signal between 395 eV and 405 eV in a high-resolution XPS spectrum (Figure 5d). The N1s high-resolution scan could be fitted into two peaks with binding energies of 401.94 eV and 399.31 eV, which were attributed to C-N and $C\text{-}N^+$, respectively. And no characteristic signal for iron (Fe 2p) between 710 eV and 740 eV in the high-resolution XPS spectrum was observed, confirming that there was no leakage of $Fe_3O_4$ on the surface of C18−PS−DVB−$Fe_3O_4$.

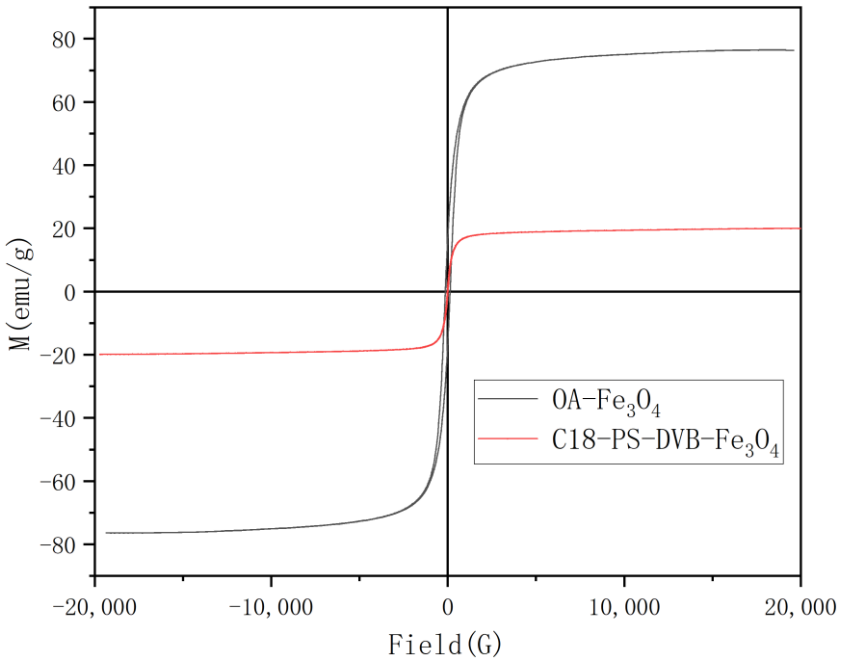


**Figure 4.** Magnetization curves of $Fe_3O_4$ and C18−PS−DVB−$Fe_3O_4$ nanoparticles.

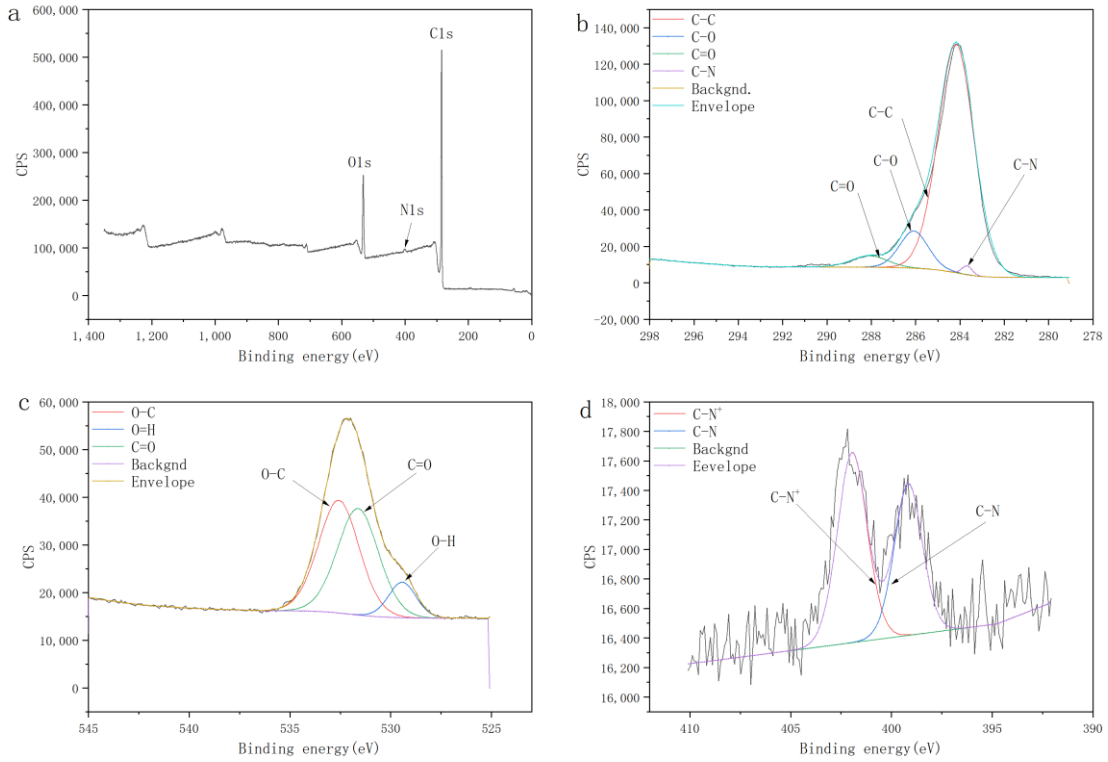


**Figure 5.** X-ray photoelectron spectroscopy (XPS) analysis (**a**), the fit of the C1s XPS spectrum (**b**), the fit of the O1s XPS spectrum (**c**), the fit of the N1s XPS spectrum (**d**).

### 2.1.4. Specific Surface Area Analysis

To further investigate the entirely porous natures of C18−PS−DVB−$Fe_3O_4$, $N_2$ adsorption–desorption measurements were performed (as shown in Figure S1a). The $N_2$ adsorption isotherm accords with the type III isotherm. The test results showed that the specific surface area of this material was 372.00 $m^2/g$. From the pore size distribution calculated by the desorption branch of the isotherm of the particles by the BJH method

(Figure S1b), the pore size range of the material was between 0 nm and 70 nm, and the mesopore of 3.0–4.0 nm was dominant, which showed that the material has a good pore structure (including micropores, mesopores, and macropores).

In addition, it was compared with the materials without C18 modification (Figure S2). The specific surface area of PS−DVB−$Fe_3O_4$ was 415.25 $m^2/g$, which was lower than that of C18 modified, which may be due to the blocking of some voids after C18 grafting.

### 2.1.5. FTIR Analysis

In order to further identify the functional groups on the surface of the synthesized sample, FTIR test was used, as shown in Figure 6. The tensile vibration peak at 3420 $cm^{-1}$ corresponds to the -OH functional group. The absorption peak at 2852 $cm^{-1}$ belongs to methylene, and the peak intensity of PS−DVB−$Fe_3O_4$ at this position is significantly weaker than that of C18−PS−DVB−$Fe_3O_4$, which was mainly due to the rich methylene ($(-CH_2)_{17}$) in N, N-dimethyloctadecylamine. The absorption peak at 1244 $cm^{-1}$ was the epoxy group, and the peak intensity of PS−DVB−$Fe_3O_4$ at this position is significantly stronger than that of C18−PS−DVB−$Fe_3O_4$ because the C18 functional group was grafted by the epoxy ring opening reaction. According to the increase in the intensity of the methylene peak and the decrease in the intensity of the epoxy group peak, it was shown that the C18 functional group was successfully grafted.

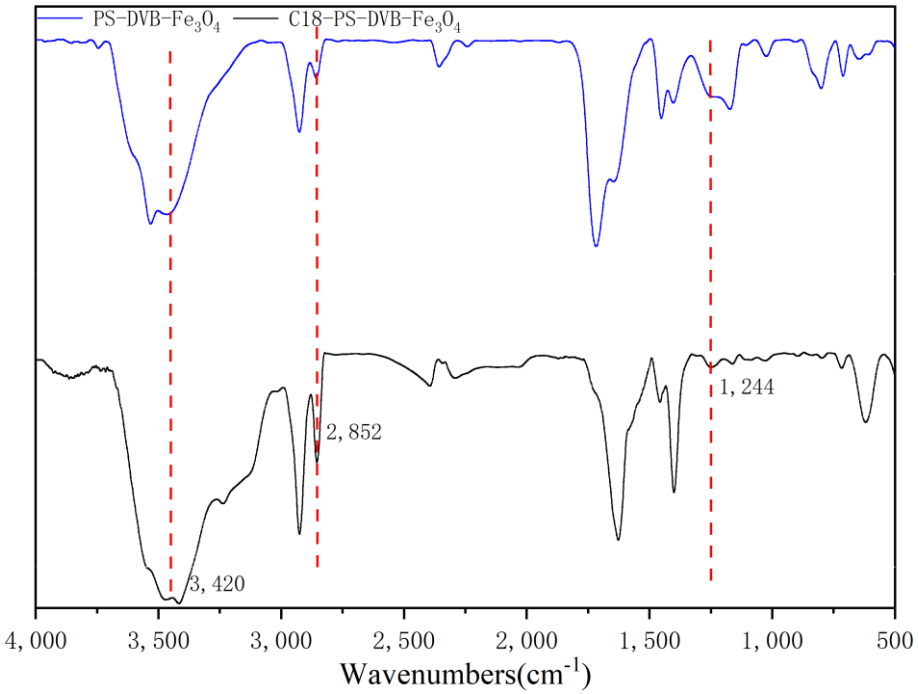


**Figure 6.** FTIR analysis of PS−DVB−$Fe_3O_4$ and C18−PS−DVB−$Fe_3O_4$.

### 2.1.6. Nitrogen Content Analysis

The Elementar Vario EL element analyzer was used to analyze the nitrogen content of the sample, and the results are shown in Table 1. In the synthesis process of C18 functionalized nano $Fe_3O_4$ magnetic polymer materials, GMA is the only oxygen source, and N, N-dimethyloctadecylamine was the only nitrogen source. Therefore, the grafting rate of C18 functional groups can be calculated by detecting the oxygen and nitrogen content in the materials. It could be concluded from this Table that the content of O atoms in the non-functionalized nano-magnetic polymer composite was 9.6%, that the content of GMA in the material was 0.40 g/g, and that there was 2.546 mmol of the epoxy group in the 1.0 g magnetic polymer composite. After C18 functionalization, O content decreased to 8.5%, while N content was 1.5%. It can be calculated that the contents of GMA and N,

N-dimethyloctadecylamine in the 1.0 g C18 functionalized magnetic polymer composite were 0.25 g/g and 0.30 g/g, respectively. In the 1.0 g magnetic polymer composite, the C18 functional group exists at 1.766 mmol and the epoxy group exists at 1.035 mmol. It can be concluded that the grafting rate of the C18 functional group was 58.6%.

**Table 1.** Nitrogen analysis of C18−PS−DVB−$Fe_3O_4$.

| Material | Gross Mass (g) | N% | O% | Epoxy Group Content (mmol) | N, N-Dimethyloctadecylamine |
|---|---|---|---|---|---|
| PS−DVB−$Fe_3O_4$ | 1.0 | / | 12.23 | 2.546 | / |
| C18−PS−DVB−$Fe_3O_4$ | 1.0 | 1.45 | 8.46 | 1.766 | 1.035 |

### *2.2. C18−PS−DVB−$Fe_3O_4$ Mag-dSPE Procedure and Its Optimization*

In this work, C18−PS−DVB−$Fe_3O_4$ nanocomposites were used as adsorbents for 11 food additives, and then the target substances were extracted from environmental water samples by the Mag-dSPE procedure. In this process, the type and concentration of the eluent, amount of adsorbent, pH of the water sample, and volume of the water sample will affect the recovery of the analyte.

#### 2.2.1. Optimization of Elution Solvent

The selection of a suitable elution solvent was an important aspect of improving the extraction efficiency. The ideal elution solvent can completely elute the analyte from the surface of the extraction material. In this study, several solutions of formic acid/methanol (1.0%, $v/v$), ammonia/methanol (1.0%, $v/v$), 2.0 mmol/L ammonium acetate in methanol, 5.0 mmol/L ammonium acetate in methanol, 10.0 mmol/L ammonium acetate in methanol, 15.0 mmol/L ammonium acetate in methanol, 20.0 mmol/L ammonium acetate in methanol, and 25.0 mmol/L ammonium acetate in methanol were studied. The results are shown in Figures 7 and 8. The elution effect of the 2.0 mmol/L ammonium acetate–methanol solution was obviously better than formic acid/methanol (1.0%, $v/v$) and ammonia/methanol (1.0%, $v/v$). Using 2.0 mmol/L ammonium acetate in methanol, the recoveries of 11 food additives were 15.62–24.3%. The possible reason was that the mixture of ammonium acetate and methanol destroys the electrostatic force between C18−PS−DVB−$Fe_3O_4$ and analytes. Compared with the ammonium acetate solution of 2.0 mmol/L, using the ammonium acetate solution of 20.0 mmol/L as the eluent, the elution effect of 11 kinds of food additives was the best, and the recoveries were 89.8–108.0%. It may be explained that the higher the concentration of ammonium acetate, the greater the destruction intensity of the electrostatic force between C18−PS−DVB−$Fe_3O_4$ and the analyte.

#### 2.2.2. Optimization of Adsorbent Dosage

The control of the adsorption dose has a great influence on the adsorption effect of the target substance. If the adsorption dose is too small, the target can not be completely adsorbed, and if the adsorption dose is too much, there will be too many irreversible points on the surface of the adsorbent so that the adsorbed target can not be eluted successfully, thus affecting the elution efficiency. In this paper, adsorbent dosages such as 10 mg, 20 mg, 30 mg, 40 mg, and 50 mg are selected for research. According to the experiment, the recoveries of 11 kinds of food additives were obtained. As shown in Figure 9, the trend of recovery was obvious when the amount of adsorbent was in the range of 10–50 mg. The adsorption effect was best when the amount of adsorbent was 40 mg, and the recoveries of 11 food additives were 88.2–105.2%. When the amount of adsorbent increased to 50 mg, the recovery did not change significantly. Therefore, the adsorbent of 40 mg is the best dosage.

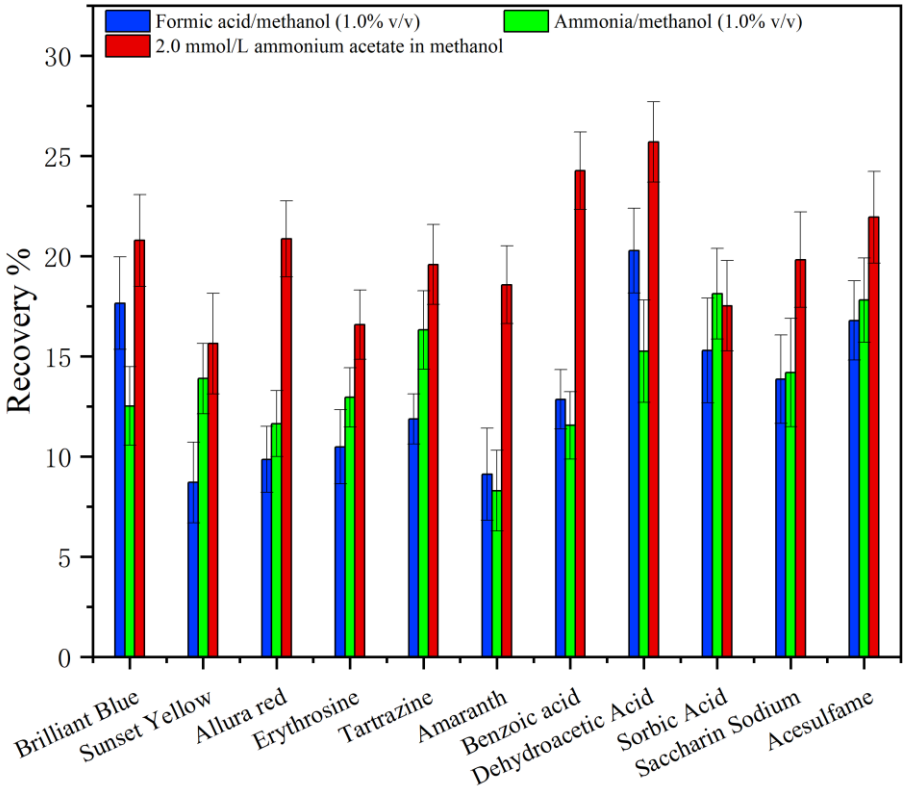


**Figure 7.** Effect of the type of desorption solvent on the recovery ($n$ = 6).

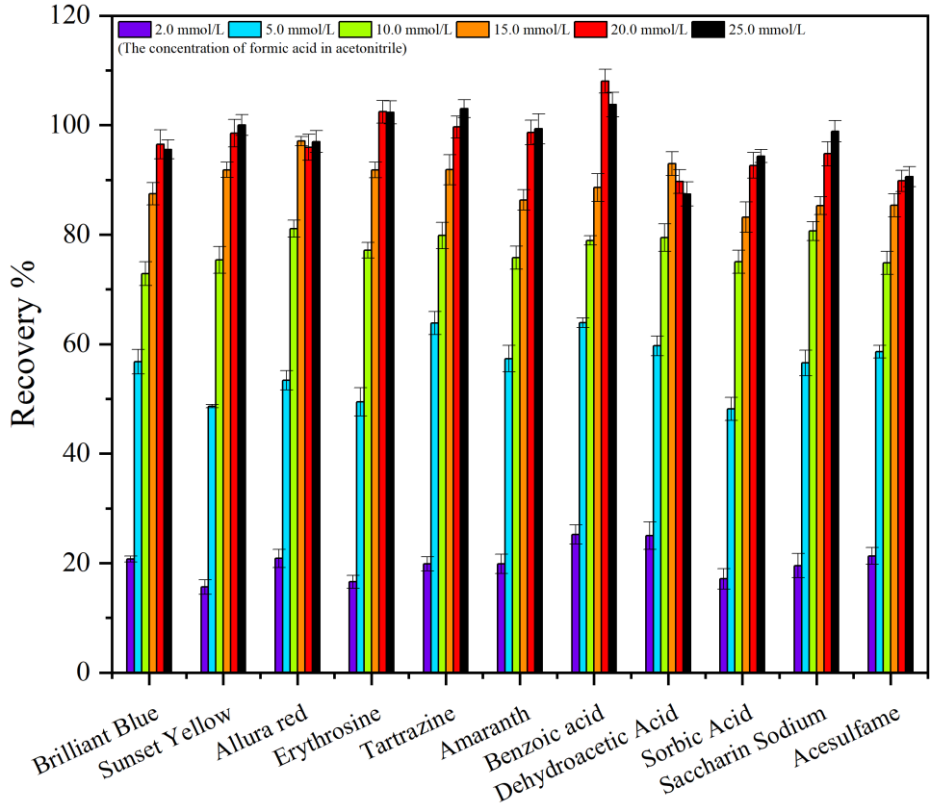


**Figure 8.** Influence of different concentrations of the ammonium acetate–methanol solution on the recovery ($n$ = 6).

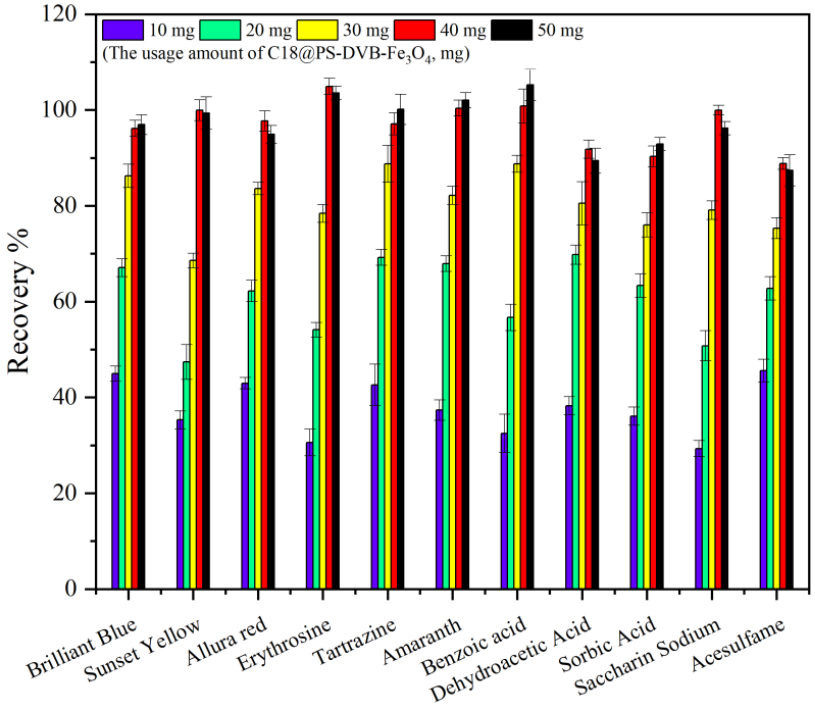


**Figure 9.** Effect of adsorbent dosage on the recovery ($n$ = 6).

### 2.2.3. Optimization pH of Water Sample

Various pH values from 3.0 to 11.0 were used to optimize the Mag-dSPE procedure, and the results were shown in Figure 10. It indicated that, with the increasing of pH values from 3.0 to 11.0, there was no significant effect on the recovery of the target analytes, and the recoveries were in the range of 70.1–101%. With the increasing of pH values from 5.0 to 7.0, the satisfactory recoveries of the 11 food additives increased slightly. Above pH 7.0, the recoveries of 11 food additives decreased with the increase in pH within the studied pH range. Above all, 7.0 was chosen as the pH value for the investigations that followed.

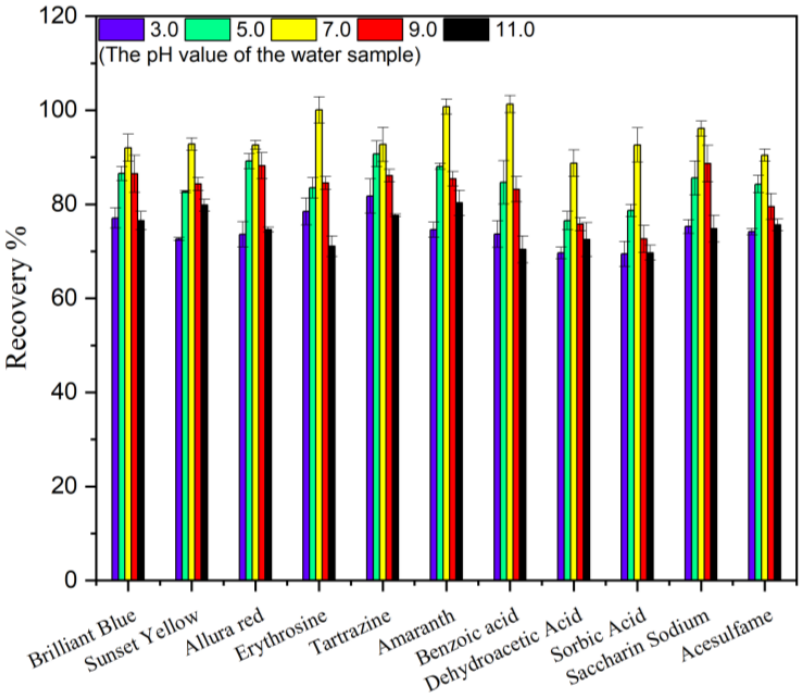


**Figure 10.** Effect of pH on the recovery ($n$ = 6).

2.2.4. Optimization of Volume of Water Sample

To obtain reliable analytical results and a high enrichment factor, obtaining satisfactory recoveries of the target substance from a large volume of sample solutions is very important. Maximum volumes ranging from 20 mL to 200 mL were studied. Following the experimental procedure, the recoveries of 11 food additives at different volumes were obtained, and the results indicate that the maximum volume was as high as 100 mL with a recovery >88.7% (Figure 11). Therefore, 100 mL of the sample solution was adopted for the preconcentration of 11 food additives from sample solutions. A high enrichment factor of 100 times was obtained because the final elute solution was 1.0 mL in these experiments.

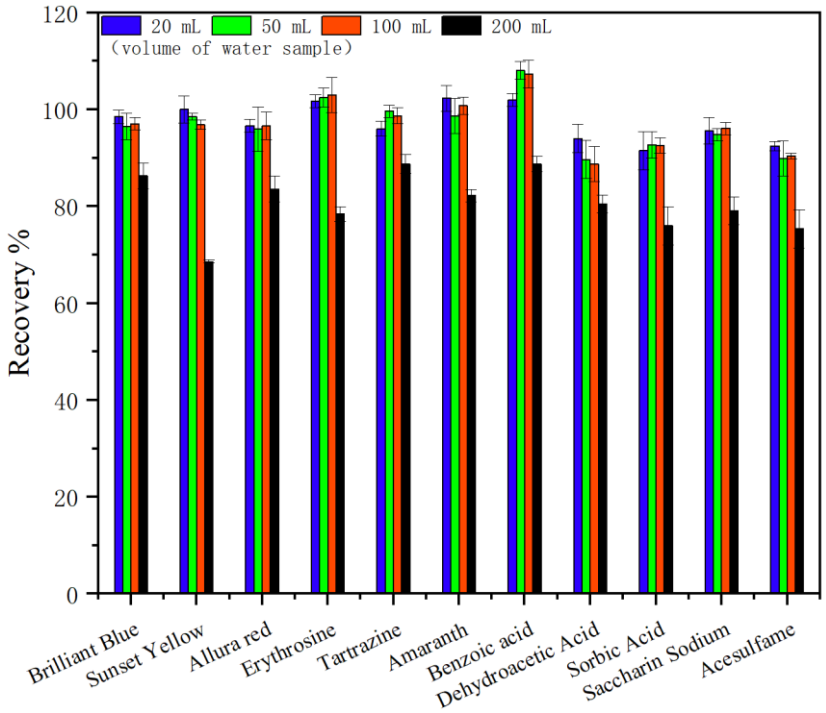


**Figure 11.** Effect of volume on the recovery ($n$ = 6).

Finally, the optimum conditions were determined as follows: 40 mg C18−PS−DVB−$Fe_3O_4$ was used as an adsorbent to enrich 11 kinds of food additives by 100 times, then 20 mmol/L ammonium acetate solution was used as an eluent to elute the nanoparticles adsorbed with food additives, and then these were analyzed by HPLC. The obtained chromatogram is shown in Figure 12.

*2.3. Analytical Performance of the Method*

Under the magnetic solid phase extraction procedure, 11 kinds of food additives were analyzed by HPLC. It can be seen from Table 2 that 11 kinds of food additives were well enriched in the pretreatment stage. The linear range of 11 kinds of food additives was 0.1–10 μg/mL. The linear correlation coefficients were all above 0.9990. LODs and LOQs were 0.6–3.1 μg/L and 2.0–10.0 μg/L, respectively. The RSD was evaluated by measuring the solution in three groups of parallel experiments. The intra-day and inter-day RSD values of 11 food additives were less than 5.9% and 8.8%, respectively.

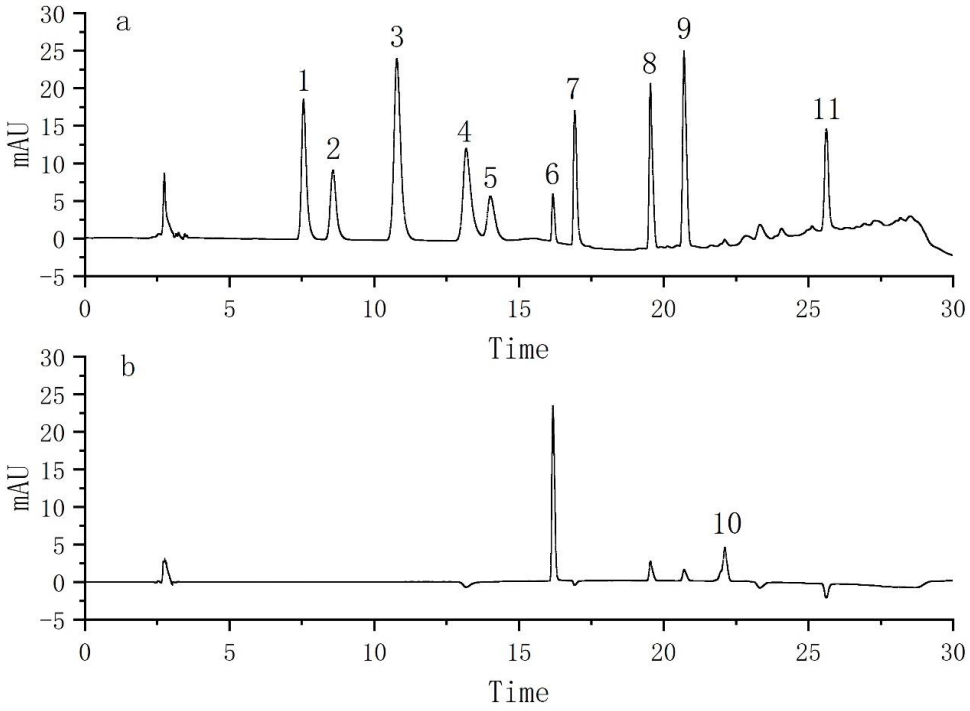


**Figure 12.** Chromatographic separation diagram of 11 food additives. The wavelength of 240 nm (**a**); The wavelength of 410 nm (**b**). (1) Acesulfame; (2) benzoic acid; (3) sorbic acid; (4) dehydroacetic acid; (5) saccharin sodium; (6) tartrazine; (7) amaranth; (8) sunset yellow; (9) Allura red; (10) brilliant blue; (11) erythrosine.

**Table 2.** Linear Equation, LODs, and RSD of 11 food additives ($n$ = 6).

| Target | Linear Range (μg/mL) | Linear Equation | $R^2$ | LOD (μg/L) | LOQ (μg/L) |
|---|---|---|---|---|---|
| Acesulfame | 0.1–10 | Y = 22.86X + 7.068 | 0.9991 | 2.3 | 7.6 |
| Benzoic Acid | 0.1–10 | Y = 15.31X + 3.012 | 0.9994 | 2.0 | 6.6 |
| Sorbic Acid | 0.1–10 | Y = 20.27X + 5.462 | 0.9998 | 1.8 | 5.9 |
| Dehydroacetic Acid | 0.1–10 | Y = 6.585X + 8.065 | 0.9992 | 2.7 | 8.9 |
| Saccharin Sodium | 0.1–10 | Y = 7.042X + 1.530 | 0.9992 | 2.9 | 9.6 |
| Tartrazine | 0.1–10 | Y = 2.327X + 0.5170 | 0.9997 | 3.0 | 9.9 |
| Amaranth | 0.1–10 | Y = 15.720X + 1.708 | 0.9995 | 2.3 | 7.6 |
| Sunset Yellow | 0.1–10 | Y = 19.166X + 3.887 | 0.9995 | 1.2 | 4.0 |
| Allura Red | 0.1–10 | Y = 24.529X + 5.627 | 0.9993 | 0.6 | 2.0 |
| Brilliant Blue | 0.1–10 | Y = 18.27X + 1.075 | 0.9991 | 3.1 | 10.0 |
| Erythrosine | 0.1–10 | Y = 13.25X − 0.2473 | 0.9996 | 2.4 | 7.9 |

### *2.4. Regeneration and Reproducibility of C18−PS−DVB−$Fe_3O_4$*

Using the same batch of C18−PS−DVB−$Fe_3O_4$ particles, the regeneration and stability of C18−PS−DVB−$Fe_3O_4$ particles as Mag-dSPE adsorbents were studied through six adsorption–desorption experiments. Before adsorption, the adsorbed particles will be washed with a desorption agent three times to remove the residual desorption agent in the last desorption process. As shown in Figure S3, C18−PS−DVB−$Fe_3O_4$ can be reused up to five times and the extraction efficiency will not be significantly reduced, but, in the sixth adsorption process, the adsorption performance will be greatly reduced. In addition, the preparation reproducibility of C18−PS−DVB−$Fe_3O_4$ was evaluated, and the results showed that the RSD of the three batches of adsorbents for 11 food additives were all less than 8.8%. Therefore, C18−PS−DVB−$Fe_3O_4$ had good regeneration performance and stability, and its preparation process also had good repeatability.

Furthermore, the preparative reproducibility of C18−PS−DVB−$Fe_3O_4$ was evaluated. The results show that the relative deviations of the recoveries for 11 food additives by using six batches of the sorbents are in the range of 3.7–9.4%. This indicates that the preparation procedure of C18−PS−DVB−$Fe_3O_4$ has good repeatability and reproducibility.

### *2.5. Method Validation and Real Sample Analysis*

To explore the practicability of the established method, it was applied to detect 11 food additives in environmental water samples. Under optimal conditions, standard solutions of food additives synthesized in 11 were added to all samples to evaluate the matrix effects. Four groups of experiments were set up; the first group was the original water sample, the standard solution addition in the second group was 1.6 μg/L, the standard solution addition in the third group was 16 μg/L, and the standard volume addition in the fourth group was 80 μg/L. The obtained results are shown in Table 3. The recoveries were 86.53–106.32%, the inter-day RSD was 0.8–8.8%, and the intra-day RSD was 0.4–5.9%. Furthermore, Benzoic acid, temptation red, and erythrin were positive in the river water samples. The detected concentrations were 4.1 μg/L, 1.2 μg/L, and 7.0 μg/L, respectively. Therefore, the detection of food additives in environmental water samples is very necessary.

**Table 3.** Content, recovery rate, and relative standard deviation of 11 food additives in environmental water samples ($n$ = 6).

| Analytes | Sample Concentration (μg/L) | Added (μg/L) | Recovery % | RSD % | |
|---|---|---|---|---|---|
| | | | | Inter-Day | Intra-Day |
| Acesulfame | — | 1.6 | 97.60 | 1.5 | 2.3 |
| | | 16.0 | 96.45 | 3.8 | 5.8 |
| | | 80.0 | 99.21 | 2.9 | 0.4 |
| Benzoic acid | 4.1 | 1.6 | 98.02 | 5.8 | 3.8 |
| | | 16.0 | 101.53 | 0.8 | 4.2 |
| | | 80.0 | 99.63 | 6.5 | 5.5 |
| Sorbic acid | — | 1.6 | 98.25 | 2.9 | 1.9 |
| | | 16.0 | 95.65 | 3.2 | 3.6 |
| | | 80.0 | 96.02 | 1.8 | 1.1 |
| Dehydroacetic acid | — | 1.6 | 102.31 | 2.9 | 1.6 |
| | | 1.6.0 | 106.32 | 3.7 | 4.2 |
| | | 80.0 | 105.27 | 4.1 | 5.9 |
| Saccharin Sodium | — | 1.6 | 98.24 | 5.8 | 1.3 |
| | | 16.0 | 97.35 | 1.9 | 5.1 |
| | | 80.0 | 100.62 | 4.1 | 4.8 |
| Tartrazine | — | 1.6 | 99.32 | 3.2 | 3.7 |
| | | 16.0 | 101.52 | 6.2 | 1.2 |
| | | 80.0 | 99.61 | 4.7 | 1.4 |
| Amaranth | — | 1.6 | 99.45 | 2.3 | 3.7 |
| | | 16.0 | 102.90 | 1.5 | 2.2 |
| | | 80.0 | 104.80 | 6.9 | 4.1 |
| Sunset Yellow | — | 1.6 | 91.40 | 8.8 | 2.7 |
| | | 16.0 | 90.55 | 4.7 | 5.6 |
| | | 80.0 | 93.93 | 3.6 | 0.5 |
| Allura Red | 1.2 | 1.6 | 93.90 | 1.1 | 5.5 |
| | | 16.0 | 94.77 | 3.9 | 3.8 |
| | | 80.0 | 95.63 | 2.3 | 1.2 |
| Brilliant Blue | — | 1.6 | 95.10 | 3.8 | 0.8 |
| | | 16.0 | 88.23 | 4.1 | 0.7 |
| | | 80.0 | 90.52 | 2.6 | 4.2 |
| Erythrosine | 7.0 | 1.6 | 89.71 | 1.3 | 4.8 |
| | | 16.0 | 86.53 | 1.7 | 0.9 |
| | | 80.0 | 87.84 | 7.5 | 3.4 |

### *2.6. Compared with Other Methods*

The performance of an extraction method based on C18−PS−DVB−$Fe_3O_4$ was compared with previously reported extraction methods for the determination of food additives. As can be seen in Table 4, the proposed method was demonstrated to have lower LODs values compared to other methods, and also had good RSD values and recovery.

**Table 4.** Comparison of the proposed method with other previously reported methods for the determination of food additives in different samples.

| Sample | Sorbent | Detection Method | Recovery (%) | RSD (%) | LOD (μg/L) | Ref. |
|---|---|---|---|---|---|---|
| The aqueous food | Silica C18 cartridge | LC-DAD | 78–104% | 2.0–7.7 | 34,000–71,000 | [41] |
| Food packages | Silica C18 cartridge | HPLC-UV | 67.48–108.5% | 2.7–9.8 | 900–1720 | [42] |
| Plastic packaging | $Fe_3O_4$@CTAB | HPLC-UV | 84.5–98.9% | 0.4–2.4 | 90–170 | [43] |
| Soft drink samples | $Al_2O_3$ | HPLC-DAD | 90.4–109.2 | 0.7–5.1 | 9.5–9.9 | [44] |
| Drink samples | $Fe_3O_4$@rGO | HPLC | 88.9–95.9 | <2.7 | 10.0–15.9 | [45] |
| Liquor samples | Decanoic acid coated-$Fe_3O_4$ NPs | HPLC | 88.9–105.4 | 2.9–3.8 | 0.9–2.4 | [46] |
| River water | PS−DVB−$Fe_3O_4$ | HPLC-DAD | 43.6–67.3 | 2.5–9.8 | 15.1–26.7 | In this work |
| River water | C18−PS−DVB−$Fe_3O_4$ | HPLC-DAD | 86.5–106.3 | 0.4–8.8 | 0.6–3.1 | In this work |

In addition, this study also compared it with PS−DVB−$Fe_3O_4$ without C18 modification. The results showed that the materials without C18 modification were inferior to those without C18 modification in terms of detection limit and recovery. In the process of adsorption, PS−DVB−$Fe_3O_4$ belongs to physical adsorption and had no selectivity, while C18−PS−DVB−$Fe_3O_4$ belongs to chemical adsorption and had a certain selectivity, so the adsorbed material was purer, thus reducing the matrix effect and increasing the detection accuracy of the instrument.

## 3. Experimental

### *3.1. Reagents and Materials*

Ferric chloride hexahydrate ($FeCl_3 \cdot 6H_2O$), sodium acetate (NaAc), oleic acid (OA), ethylene glycol (EG), polyvinyl pyrrolidone (PVP), styrene (ST), divinylbenzene (DVB), 2,2′-Azobis(2-methylpropionitrile) (AIBN), sodium dodecyl sulfate (SDS), Dibutyl phthalate (DBP), polyvinyl alcohol (PVA), benzoyl peroxide (BPO), N, N-dimethyloctadecylamine, glycidyl methacrylate (GMA), and ammonium acetate of analytical grade were purchased from Sinopharm Chemical Reagent Co., Ltd. (Shanghai, China). Methanol of HPLC grade and the standard solution of acesulfame, amaranth, benzoic acid, tartrazine, saccharin sodium, sorbic acid, dehydroacetic acid, sunset yellow, allura red, brilliant blue, and erythrosine with concentrations of 1000 mg/L were purchased from Aladdin Bio-Chem Technology Co., Ltd. (Shanghai, China).

### *3.2. Equipment*

The magnetic and morphological characteristics of C18−PS−DVB−$Fe_3O_4$ were carried out by using a Lake Shore 7404 vibrating sample magnetometer (VSM) (Westerville, OH, USA) and Zeiss Supra 55 Field emission scanning electron micrographs (SEM) (Zeiss, Oberkochen, Germany). X-ray photoelectron spectroscopy (XPS) data were obtained by Thermo Escalab 250XI (Thermo Escalab, Waltham, MA, USA). The specific surface area and pore size of the adsorbent were measured and calculated by Brunner–Emmet–Teller (BET) and Barrett–Joyner–Halenda (BJH) methods (Micromeritics, Norcross, GA, USA). Furthermore, C18−PS−DVB−$Fe_3O_4$ was also analyzed by Fourier transform infrared spectroscopy (FTIR).

### *3.3. Synthesis of PS−DVB−$Fe_3O_4$*

#### 3.3.1. Synthesis of $Fe_3O_4$

The $Fe_3O_4$ nanoparticles were prepared by the solvothermal method [47]. Briefly, 2.0 g $FeCl_3 \cdot 6H_2O$ and 6.0 g NaAc were dissolved in 40 mL EG under ultrasonication, and then it was transferred to a Teflon-lined stainless steel autoclave (100 mL). Afterwards, the autoclave was heated to 200 °C and was maintained for 6 h, then cooled naturally to room temperature. Under the action of a magnetic field, the obtained $Fe_3O_4$ particles were washed with deionized water and anhydrous ethanol and were then dried in a vacuum oven at 60 °C for 12 h.

#### 3.3.2. OA Coated $Fe_3O_4$ Nanoparticles

Furthermore, 1.0 g of $Fe_3O_4$ as prepared above was dispersed in 200 mL of anhydrous ethanol. Then, 5.0 mL OA was slowly dripped at a reaction temperature of 80 °C and a stirring speed of 500 rpm. And then, the reaction lasted for 1.0 h. At the end of the reaction, under the action of a magnetic field, the obtained particles were washed with deionized water and anhydrous ethanol and then vacuum dried at 60 °C for 12 h. Save the brown particles and set them aside.

#### 3.3.3. Synthesis of PS−DVB−$Fe_3O_4$

Then, the 1.0 g $Fe_3O_4$ nanoparticles coated with oleic acid, 1.0 g PVP, 100 mL 95% ethanol-water, 6.0 g ST, and 0.8 g AIBN were uniformly mixed and transferred to a 250 mL three-neck flask. The stirring speed was 150 rpm. The reaction was carried out with nitrogen for 24 h. Then, the obtained particles were washed with deionized water and anhydrous ethanol ethylene several times under the action of a magnetic field.

Afterwards, the particles were transferred to the three-neck flask of 500 mL and added to the 20 mL SDS (0.2%, *m*/*v*) solution. DBP was added to 30 mL SDS (0.2%, *m*/*v*) solution and emulsified for 1 h and then poured into the three-neck flask at a stirring speed of 150 rpm at 30 °C for 24 h. Additionally, 2.5 g PVA, 0.8 g SDS, 0.2 g BPO, 5.0 mL GMA, 7.5 mL DVB, and 14 mL toluene were added to 250 mL deionized water, emulsified for 2 h, poured into the three-neck flask, and stirred at 30 °C. The reaction was carried out with nitrogen at 70 °C for 24 h. The obtained particles were washed several times with hot water and anhydrous ethanol under the action of a magnetic field.

#### 3.3.4. Synthesis of C18−PS−DVB−$Fe_3O_4$

Furthermore, 25 mL methanol was used as a solvent, adding 1.0 g of PS−DVB−$Fe_3O_4$ polymer composite material, and then undergoing ultrasonic dispersion for 5.0 min. Under the condition of 80 °C, condensation reflux, and 2.5 mL N, N-dimethyloctadecylamine was added to the reaction system under the stirring speed of 500 rpm for 8 h. After the reaction was completed, the C18−PS−DVB−$Fe_3O_4$ particles were washed with deionized water and then washed with anhydrous ethanol several times under the action of a magnetic field. Then, it was dried in a vacuum drying box at 60 °C for 12 h. Finally, the C18−PS−DVB−$Fe_3O_4$ nanoparticles were obtained.

### *3.4. HPLC-DAD Analysis*

The chromatographic separation was performed on a ChromCore$^{TM}$AQC18 (5 μm, 4.6 × 250 nm) by using 20 mmol/L ammonium acetate in water as eluent (A) and methanol as eluent (B) as the mobile phase. The detector wavelengths were 240 nm and 410 nm, and the temperature of the column thermostat was 20 °C. The injection volume was 10 μL. The separation was accomplished at a constant flow of 1.0 mL/min. The linear gradient conditions were shown in Table S1.

### *3.5. Method Validation*

#### 3.5.1. Standard Preparation

Stock standard solution at the concentration of 100 mg/L for acesulfame, amaranth, benzoic acid, tartrazine, saccharin sodium, sorbic acid, dehydroacetic acid, sunset yellow, allura red, brilliant blue, and erythrosine were prepared by diluting the standard solution (1000 mg/L) in ultra-pure water. Five groups of mixed standard solutions with the concentration of 0.1 μg/mL, 0.5 μg/mL, 1.0 μg/mL, 5.0 μg/mL, and 10 μg/mL were prepared by diluting the standard solution (100 mg/L) with ultra-pure water, respectively.

#### 3.5.2. Mag-dSPE Procedure

Firstly, the environmental water sample was filtered with a 0.45 μm filter membrane to remove the particles in the environmental sample. Then, 40 mg C18−PS−DVB−$Fe_3O_4$ was dispersed in 100 mL environmental sample solution and stirred for 20 min to make the analyte fully adsorbed by magnetic nanoparticles. Then, under the action of a magnetic field, the solid–liquid separation was completed. The separated particles were eluted with 20 mmol/L ammonium acetate–methanol solution (1.0 mL). The collected eluent was passed through a 0.45 μm filter membrane and transferred to the injection bottle. The final solution was injected into the HPLC system for progressive analysis.

#### 3.5.3. Validation Parameters

In this experiment, the linearity, precision, reproducibility, and accuracy of the method were evaluated. Through the analysis of the standard samples of five concentrations, the standard curves of the peak area and concentration were obtained. The obtained standard curve was used to correct the spiked samples. When the signal-to-noise ratio (S/N) was 3 and 10, respectively, the LOQs and LODs values were estimated according to the baseline noise method. The accuracy of the method was expressed by recovery, and the precision was expressed by intra-day and inter-day RSD. The inter-day RSD was obtained by repeating experiments for 6 times in 6 days. The intra-day RSD was obtained by repeating experiments for 6 times in one day.

## 4. Conclusions

In summary, a novel magnetic nanomaterial of C18−PS−DVB−$Fe_3O_4$ was prepared. And C18−PS−DVB−$Fe_3O_4$ was used as an adsorbent of Mag-dSPE and then combined with high-performance liquid chromatography. This method was used to detect 11 food additives in environmental water samples. Under the optimum conditions, the recovery rate of 11 food additives in environmental water samples was between 86.53 and 106.32%, and the LODs were below 3.1 μg/L. This study shows that this material can effectively enrich trace food additives from environmental water samples and has potential application value. However, C18−PS−DVB−$Fe_3O_4$ still needs improvement in some areas, such as the particle uniformity not being good enough. After that, the research direction can adjust the particle size of C18−PS−DVB−$Fe_3O_4$ and prepare uniform nanoparticles. Then, it will be used as a substitute for silicon-based materials for the filling of chromatographic columns.

**Supplementary Materials:** The following supporting information can be downloaded at https://www.mdpi.com/article/10.3390/molecules29153675/s1, Figure S1: Nitrogen adsorption–desorption isotherms of C18−PS−DVB−$Fe_3O_4$ (a), The corresponding pore size distribution curves of C18−PS−DVB−$Fe_3O_4$ (b). Figure S2: Nitrogen adsorption–desorption isotherms of PS−DVB−$Fe_3O_4$. Figure S3: Reusability of C18−PS−DVB−$Fe_3O_4$ for extraction of synthetic food additives ($n$ = 6), Table S1: Mobile phase gradient elution condition.

**Author Contributions:** Writing—original draft preparation, C.L. and W.-X.L.; supervision, S.Z.; writing—review and editing, Y.-G.Z. and M.-L.Y.; funding acquisition, Y.-G.Z. All authors have read and agreed to the published version of the manuscript.

**Funding:** We would like to thank the Zhejiang Provincial Key Research and Development Project (No. 2024C03231), Talents program of Zhejiang Shuren University (KXJ0522109). The funders had no role in study design, data collection and analysis, decision to publish, or preparation of the manuscript.

**Institutional Review Board Statement:** Not applicable.

**Informed Consent Statement:** Not applicable.

**Data Availability Statement:** Details are available from authors.

**Conflicts of Interest:** The authors declare no conflict of interest.

## References

1. Sharafati Chaleshtori, R.; Golsorkhi, F. Determination of synthetic colors in some locally available foods of kashan city, Iran. *Int. Arch. Health Sci.* **2016**, *3*, 61–66. [CrossRef]
2. Minioti, K.S.; Sakellariou, C.F.; Thomaidis, N.S. Determination of 13 synthetic food colorants in water-soluble foods by reversed-phase high-performance liquid chromatography coupled with diode-array detector. *Anal. Chim. Acta* **2007**, *583*, 103–110. [CrossRef]
3. Palianskikh, A.I.; Sychik, S.I.; Leschev, S.M.; Pliashak, Y.M.; Fiodarava, T.A.; Belyshava, L.L. Development and validation of the HPLC-DAD method for the quantification of 16 synthetic dyes in various foods and the use of liquid anion exchange extraction for qualitative expression determination. *Food Chem.* **2022**, *369*, 130947. [CrossRef] [PubMed]
4. Nowak, P.M. Simultaneous quantification of food colorants and preservatives in sports drinks by the high performance liquid chromatography and capillary electrophoresis methods evaluated using the red-green-blue model. *J. Chromatogr. A* **2020**, *1620*, 460976. [CrossRef] [PubMed]
5. Jung, H.J.; Song, Y.S.; Kim, K.; Lim, C.J.; Park, E.H. Assessment of the anti-angiogenic, anti-inflammatory and antinociceptive properties of ethyl vanillin. *Arch. Pharm. Res.* **2010**, *33*, 309–316. [CrossRef]
6. Floriano, J.M.; da Rosa, E.; do Amaral, Q.D.F.; Zuravski, L.; Chaves, P.E.E.; Machado, M.M.; de Oliveira, L.F.S. Is tartrazine really safe? In silico and ex vivo toxicological studies in human leukocytes: A question of dose. *Toxicol Res.* **2018**, *7*, 1128–1134. [CrossRef] [PubMed]
7. Esimbekova, E.N.; Asanova, A.A.; Deeva, A.A.; Kratasyuk, V.A. Inhibition effect of food preservatives on endoproteinases. *Food Chem.* **2017**, *235*, 294–297. [CrossRef]
8. Lakshmi, U.R.; Srivastava, V.C.; Mall, I.D.; Lataye, D.H. Rice husk ash as an effective adsorbent: Evaluation of adsorptive characteristics for indigo carmine dye. *J. Environ. Manag.* **2009**, *90*, 710–720. [CrossRef]
9. Ma, Y.; Zhang, G.; Pan, J. Spectroscopic studies of DNA interactions with food colorant indigo carmine with the use of ethidium bromide as a fluorescence probe. *J. Agric. Food Chem.* **2012**, *60*, 10867–10875. [CrossRef]
10. Chauhan, S.S.; Sachan, D.K.; Parthasarathi, R. FOCUS-DB: An online comprehensive database on food additive safety. *J. Chem. Inf. Model.* **2021**, *61*, 202–210. [CrossRef]
11. Alreda Akkar, S.A.; Muslim Mohammed, S.A. The feasibility of emulsion liquid membrane for the extraction of organic acids from wastewater. *IOP Conf. Ser. Mater. Sci. Eng.* **2021**, *1076*, 012021.
12. Brauch, H.-J.; Remmler, F.; Skark, C.; Storck, F.R. Environmental fate and behavior of acesulfame in laboratory experiments. *Water Sci. Technol.* **2016**, *74*, 2832–2842.
13. Soylak, M.; Unsal, Y.E.; Tuzen, M. Spectrophotometric determination of trace levels of allura red in water samples after separation and preconcentration. *Food Chem. Toxicol.* **2011**, *49*, 1183–1187. [CrossRef] [PubMed]
14. Zhang, H.; Cheng, M.; Jiang, X. Determination of benzoic acid in water samples by ionic liquid cold-induced aggregation dispersive LLME coupling with LC. *Chromatographia* **2010**, *72*, 1195–1199. [CrossRef]
15. Arbelaez, P.; Borrull, F.; Pocurull, E.; Marce, R.M. Determination of high-intensity sweeteners in river water and wastewater by solid-phase extraction and liquid chromatography-tandem mass spectrometry. *J. Chromatogr. A* **2015**, *1393*, 106–114. [CrossRef] [PubMed]
16. Wu, M.; Qian, Y.; Boyd, J.M.; Hrudey, S.E.; Le, X.C.; Li, X.F. Direct large volume injection ultra-high performance liquid chromatography-tandem mass spectrometry determination of artificial sweeteners sucralose and acesulfame in well water. *J. Chromatogr. A* **2014**, *1359*, 156–161. [CrossRef] [PubMed]
17. Boyaci, E.; Gorynski, K.; Viteri, C.R.; Pawliszyn, J. A study of thin film solid phase microextraction methods for analysis of fluorinated benzoic acids in seawater. *J. Chromatogr. A* **2016**, *1436*, 51–58. [CrossRef] [PubMed]
18. Imanulkhan Setyaningsih, W.; Rohman, A.; Palma, M. Development and validation of HPLC-DAD method for simultaneous determination of seven food additives and caffeine in powdered drinks. *Foods* **2020**, *9*, 1119. [CrossRef] [PubMed]
19. Jang, G.W.; Choi, S.I.; Choi, S.H.; Han, X.; Men, X.; Kwon, H.Y.; Choi, Y.E.; Lee, O.H. Method validation of 12 kinds of food dye in chewing gums and soft drinks, and evaluation of measurement uncertainty for soft drinks. *Food Chem.* **2021**, *356*, 129705. [CrossRef]
20. Aksu Donmez, O.; Dinc-Zor, S.; Asci, B.; Bozdogan, A.E. Quantitative analysis of food additives in a beverage using high performance liquid chromatography and diode array detection coupled with chemometrics. *J. AOAC Int.* **2020**, *103*, 779–783. [CrossRef]

21. Timofeeva, I.; Kanashina, D.; Stepanova, K.; Bulatov, A. A simple and highly-available microextraction of benzoic and sorbic acids in beverages and soy sauce samples for high performance liquid chromatography with ultraviolet detection. *J. Chromatogr. A* **2019**, *1588*, 1–7. [CrossRef] [PubMed]
22. So, J.S.; Lee, S.B.; Lee, J.H.; Nam, H.S.; Lee, J.K. Simultaneous determination of dehydroacetic acid, benzoic acid, sorbic acid, methylparaben and ethylparaben in foods by high-performance liquid chromatography. *Food Sci. Biotechnol.* **2023**, *32*, 1173–1183. [CrossRef] [PubMed]
23. Tungkijanansin, N.; Alahmad, W.; Nhujak, T.; Varanusupakul, P. Simultaneous determination of benzoic acid, sorbic acid, and propionic acid in fermented food by headspace solid-phase microextraction followed by GC-FID. *Food Chem.* **2020**, *329*, 127161. [CrossRef] [PubMed]
24. Dudkina, A.A.; Volgina, T.N.; Saranchina, N.V.; Gavrilenko, N.A.; Gavrilenko, M.A. Colorimetric determination of food colourants using solid phase extraction into polymethacrylate matrix. *Talanta* **2019**, *202*, 186–189. [CrossRef] [PubMed]
25. Qin, P.; Yang, Y.; Li, W.; Zhang, J.; Zhou, Q.; Lu, M. Amino-functionalized mesoporous silica nanospheres (MSN-$NH_2$) as sorbent for extraction and concentration of synthetic dyes from foodstuffs prior to HPLC analysis. *Anal. Methods* **2019**, *11*, 105–112. [CrossRef]
26. Hatamluyi, B.; Sadeghian, R.; Malek, F.; Boroushaki, M.T. Improved solid phase extraction for selective and efficient quantification of sunset yellow in different food samples using a novel molecularly imprinted polymer reinforced by $Fe_3O_4$@UiO-66-$NH_2$. *Food Chem.* **2021**, *357*, 129782. [CrossRef] [PubMed]
27. Luna Quinto, M.; Khan, S.; Picasso, G.; Taboada Sotomayor, M.D.P. Synthesis, characterization, and evaluation of a selective molecularly imprinted polymer for quantification of the textile dye acid violet 19 in real water samples. *J. Hazard. Mater.* **2020**, *384*, 121374. [CrossRef] [PubMed]
28. Zhang, Y.; Zhou, H.; Wang, Y.; Wu, X.; Zhao, Y. Simultaneous determination of seven synthetic colorants in wine by dispersive micro-solid-phase extraction coupled with reversed-phase high-performance liquid chromatography. *J. Chromatogr. Sci.* **2015**, *53*, 210–218. [CrossRef] [PubMed]
29. Zygler, A.; Wasik, A.; Namieśnik, J. Analytical methodologies for determination of artificial sweeteners in foodstuffs. *TrAC Trend. Anal. Chem.* **2009**, *28*, 1082–1102. [CrossRef]
30. Dourado, C.S.; Domingues, I.F.F.; de Oliveira Magalhaes, L.; Casarin, F.; Ribeiro, M.L.; Braga, J.W.B.; Dias, A.C.B. Optimization of a saccharin molecularly imprinted solid-phase extraction procedure and evaluation by MIR hyperspectral imaging for analysis of diet tea by HPLC. *Food Chem.* **2022**, *367*, 130732. [CrossRef]
31. Mejia, E.; Ding, Y.; Mora, M.F.; Garcia, C.D. Determination of banned sudan dyes in chili powder by capillary electrophoresis. *Food Chem.* **2007**, *102*, 1027–1033. [CrossRef]
32. Hu, K.; Qiao, J.; Zhu, W.; Chen, X.; Dong, C. Magnetic naphthalene-based polyimide polymer for extraction of sudan dyes in chili sauce. *Microchem. J.* **2019**, *149*, 104073. [CrossRef]
33. Khoshmaram, L.; Saadati, M.; Sadeghi, F. Magnetic solid-phase extraction and a portable photocolourimeter using a multi-colour light emitting diode for on-site determination of nitrite. *Microchem. J.* **2020**, *152*, 104344. [CrossRef]
34. Liu, W.X.; Song, S.; Ye, M.L.; Zhu, Y.; Zhao, Y.G.; Lu, Y. Nanomaterials with excellent adsorption characteristics for sample pretreatment: A review. *Nanomaterials* **2022**, *12*, 1845. [CrossRef] [PubMed]
35. Khani, R.; Irani, M. Mixed magnetic dispersive micro-solid phase–cloud point extraction of sunset yellow in food and pharmaceutical samples. *Chem. Sel.* **2021**, *6*, 273–278. [CrossRef]
36. Chen, H.; Deng, X.; Ding, G.; Qiao, Y. The synthesis, adsorption mechanism and application of polyethyleneimine functionalized magnetic nanoparticles for the analysis of synthetic colorants in candies and beverages. *Food Chem.* **2019**, *293*, 340–347. [CrossRef] [PubMed]
37. Pang, Y.H.; Yue, Q.; Huang, Y.Y.; Yang, C.; Shen, X.F. Facile magnetization of covalent organic framework for solid-phase extraction of 15 phthalate esters in beverage samples. *Talanta* **2020**, *206*, 120194. [CrossRef] [PubMed]
38. Jiang, H.; Li, N.; Cui, L.; Wang, X.; Zhao, R. Recent application of magnetic solid phase extraction for food safety analysis. *TrAC Trend. Anal. Chem.* **2019**, *120*, 115632. [CrossRef]
39. Fu, X.; Zhu, D.; Huang, L.; Yan, X.; Liu, S.; Wang, C. Superparamagnetic core-shell dummy template molecularly imprinted polymer for magnetic solid-phase extraction of food additives prior to the determination by HPLC. *Microchem. J.* **2019**, *150*, 104169. [CrossRef]
40. Li, P.; Huang, D.; Huang, J.; Tang, J.; Zhang, P.; Meng, F. Development of magnetic porous carbon nano-fibers for application as adsorbents in the enrichment of trace Sudan dyes in foodstuffs. *J. Chromatogr. A* **2020**, *1625*, 461305. [CrossRef]
41. Dopico-Garcia, M.S.; Lopez-Vilarino, J.M.; Gonzalez-Rodriguez, M.V. Determination of antioxidants by solid-phase extraction method in aqueous food simulants. *Talanta* **2005**, *66*, 1103–1107. [CrossRef] [PubMed]
42. Gao, Y.; Gu, Y.; Wei, Y. Determination of polymer additives-antioxidants and ultraviolet (UV) absorbers by high-performance liquid chromatography coupled with UV photodiode array detection in food simulants. *J. Agric. Food Chem.* **2011**, *59*, 12982–12989. [CrossRef] [PubMed]
43. Zhang, D.; Liu, C.; Yang, Y.L. Determination of UV absorbers and light stabilizers in food packing bags by magnetic solid phase extraction followed by high performance liquid chromatography. *Chromatographia* **2016**, *79*, 45–52. [CrossRef]

44. Li, W.J.; Zhou, X.; Tong, S.S.; Jia, Q. Poly(N-isopropylacrylamide-co-N,N′-methylene bisacrylamide) monolithic column embedded with gamma-alumina nanoparticles microextraction coupled with high-performance liquid chromatography for the determination of synthetic food dyes in soft drink samples. *Talanta* **2013**, *105*, 386–392. [CrossRef] [PubMed]
45. Wang, X.; Chen, N.; Han, Q.; Yang, Z.; Wu, J.; Xue, C.; Hong, J.; Zhou, X.; Jiang, H. Selective separation and determination of the synthetic colorants in beverages by magnetic solid-phase dispersion extraction based on a $Fe_3O_4$/reduced graphene oxide nanocomposite followed by high-performance liquid chromatography with diode array detection. *J. Sep. Sci.* **2015**, *38*, 2167–2173.
46. Wang, J.; Zhang, L.; Xin, D.; Yang, Y. Dispersive micro-solid-phase extraction based on decanoic acid coated-$Fe_3O_4$ nanoparticles for HPLC analysis of phthalate esters in liquor samples. *J. Food Sci.* **2015**, *80*, 2452–2458. [CrossRef]
47. Liu, W.X.; Zhou, W.N.; Song, S.; Zhao, Y.G.; Lu, Y. Preparation and Characterization of Nano-$Fe_3O_4$ and Its Application for C18-Functionalized Magnetic Nanomaterials Used as Chromatographic Packing Materials. *Nanomaterials* **2023**, *13*, 1111. [CrossRef]

**Disclaimer/Publisher's Note:** The statements, opinions and data contained in all publications are solely those of the individual author(s) and contributor(s) and not of MDPI and/or the editor(s). MDPI and/or the editor(s) disclaim responsibility for any injury to people or property resulting from any ideas, methods, instructions or products referred to in the content.